Journal of Thermal Analysis and Calorimetry, Vol. 78 (2004) 251–262

THERMAL, SPECTRAL AND MAGNETIC PROPERTIES OF 2-HYDROXY-1,4-NAPHTHOQUINONE MONOXIMATES OF Ho(III), Er(III) AND Yb(III)

S. B. Jagtap[1], *R. C. Chikate*[2*], *O. S. Yemul*[3], *R. S. Ghadage*[3] *and B. A. Kulkarni*[4]

[1]Department of Chemistry, PDEA's Annasaheb Magar Mahavidyalaya, Hadapsar, Pune-411 028, India
[2]Department of Chemistry, Post-graduate and Research Center, MES Abasaheb Garware College, Karve Road, Pune-411 004, India
[3]Polymer Science & Engineering Group, Chemical Engineering Division, National Chemical Laboratory, Pashan, Pune-411 008, India
[4]Department of Chemistry, University of Pune, Pune-411 007, India

(Received July 30, 2003; in revised form February 5, 2004)

Abstract

Ho(III), Er(III) and Yb(III) complexes of 2-hydroxy-1,4-naphthoquinone-1-oxime derivatives having $[ML_3(H_2O)_2]$ are characterized using spectral and thermal decomposition studies. The thermolytic patterns suggested that they are decomposed in three distinct stages; 1st stage is related to the loss of two coordinated water molecules while one of the coordinated ligands and remaining two ligands are lost during subsequent 2nd and 3rd stages of degradation. After the 2nd stage, the structure of these complexes is reorganized reflecting that the structural associations through intermolecular hydrogen bonding network is essential for thermal stability. The kinetic parameters computed for 2nd step using the non-isothermal procedures of Coats–Redfern are applied to the respective differential thermogravimetric plots to ascertain the thermal degradation mechanism in air. The order of thermal decomposition reaction is found to be between 1–2 indicating that more than one intermediate might have simultaneously been formed. It also reveals the intermixing of 1st and 3rd stages of decomposition with the predominant 2nd stage leading to more gradual degradation. Energy of activation for 2nd stage of decomposition for these complexes is comparatively lower than those observed earlier for similar types of complexes. Other spectral data indicate oximino nitrogen and phenolato oxygen as coordination sites of 2-hydroxy-1,4-naphthoquinone monoximates.

Keywords: Coats–Redfern, energy of activation, lanthanides complexes, quinone oximes, thermal degradation

Introduction

Lanthanide complexes, as a class of compounds, have gained significant attention because of their diversified applications such as: NMR shift reagents [1], catalysts in

* Author for correspondence: E-mail: rajuchikate@rediffmail.com

1388–6150/2004/ $ 20.00

Akadémiai Kiadó, Budapest
Kluwer Academic Publishers, Dordrecht

selective hydrogenation [2], asymmetric catalyst for enantioselective chemical transformations [3], liquid crystals and surfactants [4], in plastic optical fiber lasers and amplifiers [5], electroluminescent material [6] and molecular recognition and chirality sensing of biological substrates [7].

The coordination aspects of naphthoquinone derivatives towards various transition metals have been extensively explored [8–11] for better understanding of the structural peculiarities. Moreover, these complexes are also investigated for their biological properties. The thermal decomposition patterns of naphthoquinone chelates exhibited an oxidative degradation mechanism through the formation of semiquinone form of the ligand moieties [12, 13]. The solid-state deaquation stages for cobalt(II) and copper(II) complexes of L_1 and L_2 (Fig. 1) involving *trans*- and *cis*-isomers indicated the rearrangement type of mechanism during the loss of water molecules [14, 15]. Although, thermal and spectral behaviors of lanthanide complexes were explored recently [16, 17], there are very few reports on the thermal decomposition as well as structural properties of lanthanide complexes with quinones or their oxime derivatives which include the polymeric complexes of anthraquinone [18] and embelin [19], amino-naphthoquinone [20] and halolawsone monoximes [21].

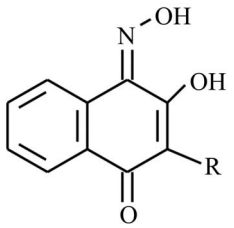

Fig. 1 Hydroxy naphthoquinone oxime ligating system.
R=H; L_1=2-hydroxy-1,4-naphthoquinone-1-oxime;
R=CH_3; L_2=3-methyl-2-hydroxy-1,4-naphthoquinone-1-oxime;
R=Cl; L_3=3-chloro-2-hydroxy-1,4-naphthoquinone-1-oxime;
R=Br; L_4=3-bromo-2-hydroxy-1,4-naphthoquinone-1-oxime;
R=I; L_5=3-iodo-2-hydroxy-1,4-naphthoquinone-1-oxime

Recently, we have reported [22, 23] the antimicrobial activities of L_1–L_5 and their complexes with Ho(III) and Er(III) wherein it was observed that the activity of parent ligand is enhanced upon complexation with these metal ions. The present communication describes the thermal and spectral properties of Ho(III), Er(III) and Yb(III) complexes of L_1–L_5 (Fig. 1).

Experimental

The hydrated Ho(III), Er(III) and Yb(III) chlorides were obtained from Indian Rare Earth's Ltd., India. All the chemicals and solvents used were of analytical grade and the solvents were purified according to standard procedure [24] before use.

Synthesis of ligands

Ligands L_1–L_5 (Fig. 1) were synthesized according to the literature reports [22, 23]. They were characterized using elemental analysis, IR, ^1H and ^{13}C NMR studies wherein it was observed that there exists *amphi*-form of oximino function [23].

Synthesis of metal chelates

A general procedure adopted for the synthesis of Ho(III), Er(III) and Yb(III) complexes was as follows:

To a hot solution of 3 mmol of oxime derivatives (L_1–L_5) in 25 mL of ethanol, an aqueous solution of 1 mmol of hexahydrates of Ho(III), Er(III) and Yb(III) chlorides was added with constant stirring. The pH of the resulting solution was maintained around 6–7 using aqueous NH_3. After refluxing for 3 h and cooled overnight, the solid mass was filtered, washed with methanol and dried under vacuum over P_2O_5. These complexes are abbreviated as Ho(III) complexes (Ho_1–Ho_5); Er(III) complexes (Er_1–Er_5) and Yb(III) complexes (Yb_1–Yb_5) with L_1–L_5, respectively.

Physical measurements

Elemental analyses were carried out using a Hosli-Holland C, H Analyzer. The magnetic susceptibility was measured [25] at room temperature on a Faraday type magnetic balance with a permanent magnetic field of 7000 G and the molecular susceptibilities were corrected for the diamagnetism of the component atoms by the use of Pascal's constants [26]. The instrument was calibrated with $Hg[Co(SCN)_4]$. The infrared spectra were recorded in nujol mulls on a Perkin Elmer FTIR spectrophotometer (Model 1600) in the range 4000–400 cm^{-1}. UV-visible spectral measurements (200–800 nm) were carried out on Shimadzu UV-300 spectrophotometer while thermogravimetric profiles were obtained on Perkin Elmer Delta (TGA-7) analyzer in air with a heating rate of 10°C min^{-1}. The X-band powder ESR spectrum at RT was recorded on Bruker ER 200D-SRC spectrometer with 100 kHz field modulation unit which was calibrated using DPPH as standard.

Results and discussion

All the poly-chelates are amorphous in nature, turmeric yellow – orange red in colour and insoluble in most of the organic solvents but are soluble in DMSO, DMF probably indicating presence of intermolecular hydrogen bonding contacts with neighboring molecules. Compositional studies (Table 1) suggested $[ML_3(H_2O)_2]$ stoichiometry with non-electrolyte nature.

Thermal studies

The non-isothermal degradation profiles of ligands L_1–L_5 and their Ho(III), Er(III) and Yb(III) complexes are examined for the decomposition characteristics. The su-

Table 1 Analytical data and magnetic moments of Ho(III), Er(III) and Yb(III) complexes of L_1–L_5

Complex	Yield/%	Elemental analysis[#]				μ_{eff}/B.M.
		C/%	H/%	N/%	M/%	
Ho_1	66.68	46.79 (47.07)	3.00 (2.90)	5.36 (5.49)	21.38 (21.55)	10.08
Ho_2	67.47	48.77 (49.08)	3.12 (3.49)	5.13 (5.20)	20.36 (20.42)	10.30
Ho_3	68.54	41.01 (41.48)	2.52 (2.20)	4.81 (4.84)	18.79 (18.98)	10.23
Ho_4	69.37	36.02 (35.96)	2.25 (1.99)	3.98 (4.19)	16.23 (16.46)	10.27
Ho_5	67.45	31.79 (31.52)	2.01 (1.68)	3.90 (3.68)	14.20 (14.43)	10.12
Er_1	71.56	47.06 (46.93)	2.76 (2.89)	5.29 (5.47)	21.55 (21.78)	9.11
Er_2	70.86	48.78 (48.94)	3.54 (3.48)	5.24 (5.19)	20.75 (20.65)	9.40
Er_3	71.89	40.93 (41.36)	2.36 (2.19)	4.65 (4.82)	19.05 (19.20)	9.28
Er_4	73.25	36.83 (37.09)	2.23 (1.97)	4.17 (4.33)	17.48 (17.21)	9.34
Er_5	68.16	31.13 (31.46)	1.91 (1.67)	3.42 (3.67)	14.39 (14.60)	9.20
Yb_1	74.12	46.12 (46.58)	2.57 (2.87)	5.18 (5.43)	22.54 (22.37)	4.13
Yb_2	73.89	48.41 (48.60)	3.49 (3.46)	5.02 (5.15)	21.25 (21.22)	4.40
Yb_3	70.52	40.82 (41.09)	2.36 (2.18)	4.59 (4.79)	19.50 (19.73)	4.29
Yb_4	72.03	36.83 (37.09)	2.07 (1.97)	4.23 (4.16)	16.90 (17.13)	4.36
Yb_5	66.14	31.24 (31.30)	1.91 (1.67)	3.50 (3.65)	15.39 (15.03)	4.21

[#]Values in the parenthesis represent the calculated %

perimposed plots of the rate of change in the mass of ligands L_1–L_5 in the temperature range 0–350°C are depicted in Fig. 2. These ligands are thermally stable (~175°C), close to their melting temperatures and on further heating a mass loss is observed corresponding to an exothermic peak. It represents the first stage of decomposition probably involving oximino function while the gradual degradation at second stage reveals the loss of remaining part of the ligand molecule. Such a behavior is found to be usually associated with quinone-oxime derivatives probably supporting the disturbance in the quinonoidal structure [27] of parent compounds.

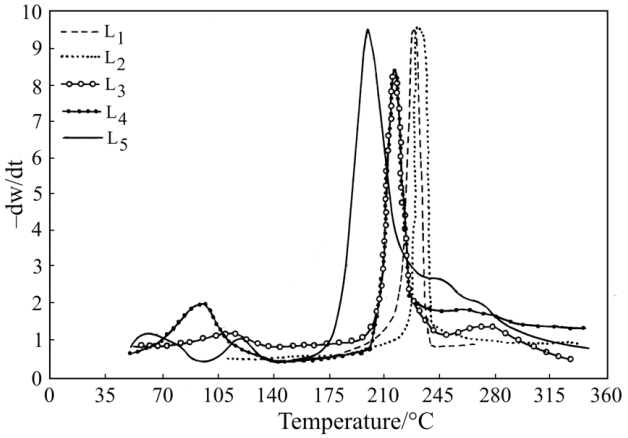

Fig. 2 DTG curves for ligands L_1–L_5

Figure 3 represents the thermal plots of Ho_3, Er_3 and Yb_3 in the temperature range 70–800°C. The inspection of thermolytic pattern of these complexes indicates that they decompose in a gradual manner, in contrast to the sharp decomposition of the corresponding ligand molecule [28, 29]. It also suggests that their degradation occurs in three distinct stages. The 1st stage of decomposition (100–180°C) indicates the loss of two coordinated water molecules. These patterns probably reflect the stronger associations of complex molecules through intermolecular hydrogen bonding contacts between coordinated water molecules and bonded ligands [8, 11]. Such a bonding can result in the formation of polymeric species leading to the decomposition of these chelates at higher temperature [20].

After the initial loss during 1st stage, very sharp break in the temperature range 190–380°C has occurred with the rapid change in the mass for the 2nd stage [30],

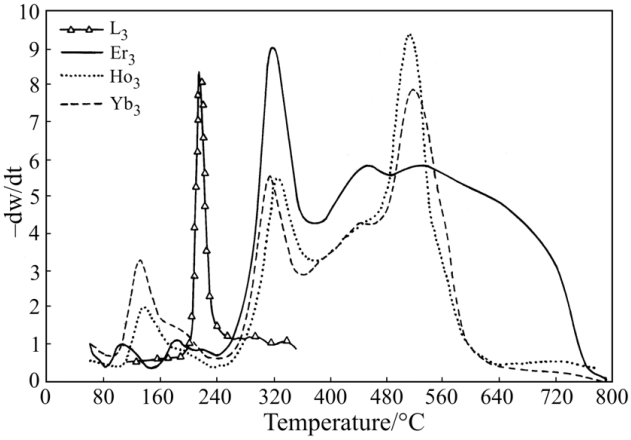

Fig. 3 DTG curves for Ho(III), Er(III) and Yb(III) complexes of L_3

which corresponds to the loss of one of the coordinated ligand molecules [12, 14]. It also indicates that the loss of coordinated water molecules during 1st stage has directly affected the structural arrangement of the complex resulting in the beginning of the onset of structural decomposition with rapid loss in volatile fragment. Moreover, the lower decomposition temperature for this stage compared to other complexes [12, 14, 28] indicates that the polymeric network is destroyed due to loss of coordinated water molecules. Finally, the total breakdown of the complex occurs during the 3rd stage (380–670°C) wherein the remaining two coordinated ligand molecules are lost with the formation of stable oxide. It is quite likely that after the loss of one of the coordinated ligand molecule, the structural arrangement of the complex is totally disturbed leading to a gradual decomposition over a very large temperature range. Simultaneously recorded DTA curves also reveal the differences in the thermal degradation of three bound ligand molecules with two endothermic peaks in the ranges 250–300 and 350–400°C. It implies that some interchanges are occurring in the structure of the complex after the loss of one of the strongly coordinated ligand molecule [31]. The overall thermal pattern for these complexes may be summarized as below:

$$[ML_3(H_2O)_2] \xrightarrow{1^{st}\ stage;\ -2H_2O} [ML_3] \xrightarrow{2^{nd}\ stage;\ -L} [ML_2] \xrightarrow{3^{rd}\ stage;\ -2L} M_2O_3$$

Er(III) complexes are thermally more stable than Ho(III) complexes and both seem to have greater stability compared to Yb(III) compounds. Such a correlation has already been established for lanthanide complexes of lawsone and juglone derivatives [32]. Complexes of L_2, however, have comparatively lower decomposition temperature. Similarly, chelates L_4 and L_5 exhibit broader thermal pattern indicating the effect of bulk on the thermal properties as well as the stability of intermediate species formed after 2nd stage of decomposition. Later on, it follows a slow and steady mass loss resembling the pattern usually observed for heavier lanthanide complex [20, 21].

It is evident from the thermogravimetric profiles that the 2nd stage of decomposition is the predominant one for all the chelates. Significantly, such a behavior is also observed for the majority of lanthanide complexes with quinone derivatives [20]. Hence, this step was selected for the evaluation of kinetic parameters using Coats–Redfern [33] non-isothermal integral equations. The DTG peak relating to this stage is separated out and corrected for area using Anderson methodology [34]. The energy of activation (E_a) for all the chelates were computed from their DTG curves. The equations used are as follows:

a) The Coats–Redfern equation 1 (CRI) [33]

$$\log\{[1-(1-\alpha)^{1-n}]/[(1-n)T^2]\} = \log\{[(AR)/(aE)]\ [1-(2RT)/E]\} - [E/2.303RT] \quad (1)$$

b) The Coats–Redfern equation 2 (CRII)

$$\log[-\ln(1-\alpha)/T^2] = \log\{[(AR)/(aE)]\ [1-(2RT)/E]\} - [E/2.303RT] \quad (2)$$

where $\alpha=(w-w_f)/(w_0-w_f)$; w_0, w_f and w are the initial mass, final mass and mass at temperature T (equivalent to the 2nd stage of decomposition).

The equation CRII is valid for reactions with reaction order n=1 and CRI is applicable for order of reaction other than unity.

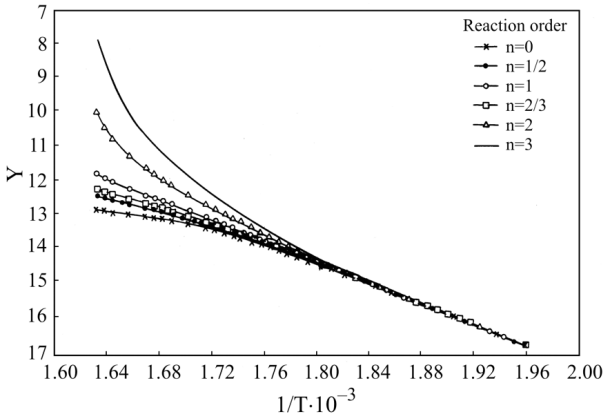

Fig. 4 Coats–Redfern plots of Er_3 at various orders of thermal reaction (2^{nd} stage)

The order parameter n is determined by above equations. The plots of left hand side (LHS) functions *vs*. $1/T$ are drawn for different values of n in the range 0–3 except for n=1; CRII was used for n=1. Figure 4 depicts the superimposed plots of LHS function of CRI or CRII *vs*. $1/T$ for Er_3 complex. For n=0, 2 and 3 (CRI), a linear relationship is not observed, whereas for n=1 (CRII), the nature of plot of log $[-\ln(1-\alpha)]$ *vs.* $1/T$ is fairly straight. This indicates that decomposition of all the chelates takes place according to first-order degradation kinetics.

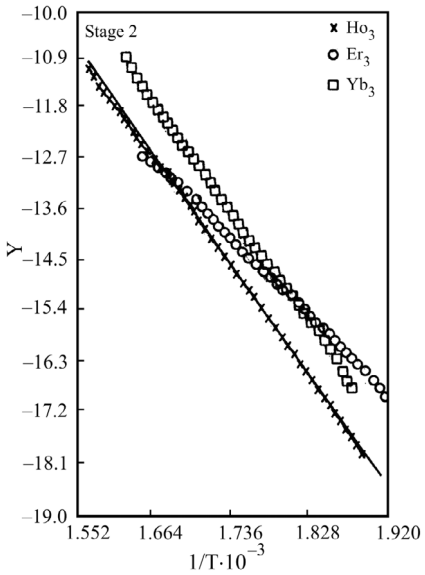

Fig. 5 Plots of log $[\ln (1-\alpha)^{-1}/T^2]$ *vs*. $1/T$ for the 2^{nd} stage decomposition process for Ho_3, Er_3 and Yb_3 complexes

The superimposed plots of log $[\ln(1-\alpha)^{-1}/T^2]$ *vs*. $1/T$ (CR plots) for Ho_3, Er_3 and Yb_3 complexes corresponding to 2nd stage of decomposition are depicted in Fig. 5. The temperature ranges and functional degradation (α) within which analyses are conducted and energy of activation are presented in Table 2.

The first order thermal decomposition kinetics of chelates has overall energy of activation (E_a) in the range of 70–246 kJ mol^{-1} (Table 2) for all the chelates of L_1–L_5. It can be seen from the data that these energies of activation are significantly lower than those reported earlier for lanthanide complexes of quinone derivatives [20, 21]. This probably reflects that the structure loses its rigidity after the loss of coordinated water molecules thus weakening the molecular association suggesting that the thermal stability is reduced. However, after the second stage of decomposition, the molecule attains some thermal stability through the structural reorganization. Similarly, it is possible that molecule may lose its polymeric nature established by coordinated water molecules and bound ligands [18–21]. These parameters also suggest that the order of thermal decomposition reaction is in between 1–2 indicating that more than one intermediate might have simultaneously been formed and subsequently undergoing a smooth decomposition leading to linear mass loss in the final stage. Moreover, values of α (mass loss at beginning and end of the stage) as well as their corresponding temperature ranges reveal that for most of the complexes, this stage of decomposition occurs in a clear and distinctive manner. However, variation in these values, particularly for Er_4 and Yb_1 is suggestive of associative decomposition mechanisms involving former and latter stages of degradation. It means that some of the complexes do not necessarily decompose in a stepwise manner; rather they exhibit a continuous and gradual degradation pattern. The intermixing of all the three stages for these complexes is also indicative of strong polymeric association thus establishing an extensive network of complex molecules. The thermolytic profiles as evidenced from Table 2 also implies that there is a strong effect of substituents on the pyrolysis of these chelates resulting in higher energy of activation for complexes of L_1 and L_3.

Infrared studies

The IR spectra of ligands and their lanthanide complexes were recorded in nujol mulls and are depicted in Table 3. The ligands exhibit medium broad bands in the range 3600–3100 cm^{-1} presumably originating from hydroxyl vibrations of oximino and phenolic functions. They are further broadened due to the overlapping of these vibrations with coordinated water molecule after chelation with Ho(III), Er(III) and Yb(III) ions [21]. Upon complexation, redistribution of electron density in quinonoid ring resulted in the shifting of (C=O) stretching frequency (1630–1600 cm^{-1}) towards lower energy side by ~20–30 cm^{-1} due to halo-substituents at C_3 position in 2-hydroxy-1,4-naphthoquinone-1-monoxime. The oxime function (C=N) was found to be involved in coordination with these metal ions as evidenced from shifting of this band (1590–1570 cm^{-1}) by a magnitude of ~40–70 cm^{-1}. The quinone absorption band (1293–1285 cm^{-1}), however, remains unaffected after complexation suggesting

Table 2 Activation energies of 2nd stage decomposition for complexes

Complex	Mass loss/%	Analysis range				E_a/ kJ mol^{-1}
		T/°C		α range		
		start	end	start	end	
Ho_1	19.3	252	370	0.03	0.89	102.9
Ho_2	10.0	173	259	0.02	0.94	98.8
Ho_3	18.6	249	371	0.02	0.91	170.9
Ho_4	20.7	222	374	0.06	0.89	170.3
Ho_5	29.4	191	347	0.01	0.84	66.4
Er_1	12.1	241	328	0.02	0.54	109.2
Er_2	14.3	237	333	0.01	0.74	131.9
Er_3	13.0	248	345	0.01	0.76	120.8
Er_4	11.3	399	443	0.40	0.93	91.5
Er_5	34.0	228	367	0.02	0.96	121.5
Yb_1	17.6	317	345	0.26	0.90	246.3
Yb_2	29.7	206	347	0.01	0.74	71.2
Yb_3	15.0	260	351	0.02	0.90	173.2
Yb_4	22.4	226	384	0.06	0.85	90.2
Yb_5	36.0	219	420	0.02	0.93	79.6

Table 3 Significant peaks (cm^{-1}) in IR spectra of Yb(III) complexes of L_1–L_5

Complex	ν(O–H)	ν(C=O)	ν(C=N)	ν(C–O)	ν(N–O)
Yb_1	3568	1586	1537	1225	1059
Yb_2	3362	1586	1518	1223	1060
Yb_3	3125	1581	1519	1225	1059
Yb_4	3315	1580	1518	1224	1060
Yb_5	3384	1581	1520	1223	1055

the presence of fully oxidized quinone form. The (C–O) stretching frequency observed around 1210 cm^{-1} in the ligand spectra was found to be present around 1190 cm^{-1} for chelates indicating phenolato oxygen as the other site of bonding for ligands. Other evidences for the complexation of 2-hydroxy-1,4-naphthoquinone monoximates are in concurrence with the earlier reports [22, 23].

Magnetic properties

The magnetic moments of lanthanide complexes of L_1–L_5 are presented in Table 1. The paramagnetic behavior of these complexes denotes the presence of unpaired electrons, which are strongly shielded by outer octet ($5s^2$, $5p^6$) both in their spin and orbital

moments. These values are found to be similar to the one reported by Van Vleck [35]. The lowering in these values may be originating from the polymeric nature of these chelates through antiferromagnetic associations of complex molecules. Such associations are established probably through intermolecular hydrogen bonding contacts between coordinated water molecules and ligands. Similar type of nature has already been established for iron(II) complex of 3-amino-2-hydroxy naphthoquinone [11] as well as with lanthanide complexes of quinone derivatives [18–21].

Electronic spectra

The electronic spectral studies were carried out in DMSO solvent. The ligands exhibit two absorption bands in the range 27248–27777 and 24390–25000 cm^{-1} which are shifted to higher energy side upon complexation while the complexes show weak *f–f* transitions with intense charge transfer absorptions. However, some of the complexes exhibit two transitions in the ranges 17800–19500 and 23600–24600 cm^{-1}, respectively for which the assignments [36] are depicted in Table 4. The red shift of hypersensitive bands has been used to calculate nephelauxetic effect ratio (β) [37], bonding parameter ($b^{1/2}$) and Sinha's parameter (δ) [38] in order to understand bonding in complexes. These values indicate extent of 4f orbital participation in complexation. As ($b^{1/2}$) values are less than unity, no appreciable overlap is present between 4f-metal orbitals and ligand π-orbitals. Also, the average value of Sinha's parameter (δ) and

Table 4 Electronic spectral data for Ho(III), Er(III) and Yb(III) complexes of L_1–L_5

Complex	λ_{max}/cm^{-1}	Assignments	Spectral parameters		
			β	δ	$b^{1/2}$
Ho_2	17857 23696	$^6H_{5/2}\rightarrow{}^6H_{3/2}$ $^6H_{5/2}\rightarrow{}^4I_{3/2}$	0.9987	1.973	0.0973
Ho_3	18518 24271	$^6H_{5/2}\rightarrow{}^6H_{3/2}$ $^6H_{5/2}\rightarrow{}^4I_{3/2}$	0.9987	1.973	0.0973
Ho_4	18518 24271	$^6H_{5/2}\rightarrow{}^6H_{3/2}$ $^6H_{5/2}\rightarrow{}^4I_{3/2}$	0.9987	1.973	0.0973
Er_2	19437 24096	$^8S_{7/2}\rightarrow{}^6P_{5/2}$ $^8S_{7/2}\rightarrow{}^6P_{3/2}$	0.9823	1.800	0.0939
Er_4	17241 23696	$^8S_{7/2}\rightarrow{}^6P_{5/2}$ $^8S_{7/2}\rightarrow{}^6P_{3/2}$	0.9713	1.834	0.0942
Er_5	18248 23923	$^8S_{7/2}\rightarrow{}^6P_{5/2}$ $^8S_{7/2}\rightarrow{}^6P_{3/2}$	0.9987	1.973	0.0973
Yb_3	19517 23809	$^4F_{5/2}\rightarrow{}^4D_{3/2}$ $^4F_{5/2}\rightarrow{}^4D_{3/2}$	0.9835	1.810	0.0956
Yb_4	19531 24096	$^4F_{5/2}\rightarrow{}^4D_{3/2}$ $^4F_{5/2}\rightarrow{}^4D_{3/2}$	0.9726	1.923	0.0906
Yb_5	18181 23815	$^4F_{5/2}\rightarrow{}^4D_{3/2}$ $^4F_{5/2}\rightarrow{}^4D_{3/2}$	0.9836	1.760	0.0951

nephelauxetic ratio (β) implies weaker covalency in metal-ligand bonding [20, 39] for the present series of complexes.

ESR studies

Although the lanthanide chelates of quinone oximes exhibit paramagnetic behavior, the analyzable EPR spectrum could not be obtained for them suggesting the strong shielding of f-electrons. Only Er_3 complex is analyzed for the structural elucidation as a representative of all the chelates. The isotropic EPR spectrum obtained for this complex with g=1.996 suggests that these electrons are not accessible for chemical bond formation. The lowering in the 'g' value as compared to free electron value suggests the polymeric nature of these complexes as has been observed in the thermogravimetric analysis [40].

Conclusions

Ho(III), Er(III) and Yb(III) complexes of 2-hydroxy-1,4-naphthoquinone-1-monoximates having $[ML_3(H_2O)_2]$ composition exhibit thermal properties corresponding to three-stage decomposition pattern. Due to the loss of two coordinated water molecules during the initial stage, it was observed that the intermolecular associations involving hydrogen-bonding contacts between free oximino hydroxyl groups and these water molecules are destroyed resulting in the formation of a less thermally stable intermediate species. Such a behavior has resulted in the lowering of the energy of activation for subsequent step; a general feature usually found to be associated with oxime complexes [41]. For some of the chelates, intermixing of these three stages of decomposition has lead to a gradual degradation with higher order of thermal reactions probably indicating the polymeric nature for these complexes. It is further corroborated with the EPR measurements of these complexes where 'g' value is found to be appreciably lowered than free electron value. Oximino hydroxyl function is involved in intermolecular hydrogen bonding network as evidenced from the broadening of hydroxyl stretch observed in IR spectrum of these complexes. The oxime ligating system has oximino nitrogen and phenolato oxygen as binding sites of L_1–L_5. Electronic absorption studies indicate negligible covalence in metal–ligand bonding.

* * *

RCC is thankful to Head, Department of Chemistry and Principal, MES Abasaheb Garware College for providing the infrastructure and constant encouragement. SBJ is thankful to UGC, New Delhi for providing Teacher Fellowship.

References

1 H. C. Aspinall, Chem. Rev., 102 (2002) 1807.
2 G. A. Molander and J. A. C. Romero, Chem. Rev., 102 (2002) 2161.
3 M. Shibasaki and N. Yoshikawa, Chem. Rev., 102 (2002) 2187.
4 K. Binnemans and C. G. Walrand, Chem. Rev., 102 (2002) 2303.

5 K. Kuriki and Y. Koike, Chem. Rev., 102 (2002) 2347.
6 J. Kido and Y. Okamoto, Chem. Rev., 102 (2002) 2357.
7 H. Tsukube and S. Shinoda, Chem. Rev., 102 (2002) 2389.
8 M. P. Mulay, P. L. Garge, S. B. Padhye, R. C. Haltiwanger, I. A. deLearie and C. G. Pierpont, J. Chem. Soc. Chem. Commun., (1987) 581.
9 S. Padhye, P. Garge and M. P. Gupta, Inorg. Chim. Acta, 152 (1988) 37.
10 P. L. Garge, S. B. Padhye and J. P. Tuchagues, Inorg. Chim. Acta, 157 (1989) 37.
11 P. Garge, R. Chikate, S. Padhye, J. M. Savariault, P. deLoth and J. P. Tuchagues, Inorg. Chem., 29 (1990) 3315.
12 S. Y. Rane, J. P. Salvekar, N. V. R. Das, P. S. Kaduskar and P. P. Bakare, Thermochim. Acta, 191 (1991) 255.
13 S. Y. Rane, S. B. Padhye, E. M. Khan and P. L. Garge, Synth. React. Inorg. Met-Org. Chem., 18 (1988) 609.
14 S. Y. Rane, S. B. Padhye, G. N. Natu, A. H. Kumar and E. M. Khan, J. Thermal Anal., 35 (1989) 2331.
15 S. Y. Rane, S. D. Gawali, A. S. Kumbhar, S. B. Padhye and P. P. Bakare, J. Therm. Anal. Cal., 55 (1999) 249.
16 A. S. M. A. Shihri and H. M. A. Fattah, J. Therm. Anal. Cal., 71 (2003) 643.
17 E. Princz, I. Szilágyi, K. Mogyorósi and I. Lábadi, J. Therm. Anal. Cal., 69 (2002) 427.
18 J. Sharma and H. B. Singh, Inorg. Chim. Acta, 133 (1987) 161.
19 M. L. Dhar and O. Singh, Inorg. Chim. Acta, 117 (1986) 187.
20 R. C. Chikate, H. A. Bajaj, A. S. Kumbhar, V. C. Kolhe and S. B. Padhye, Thermochim. Acta, 249 (1995) 239.
21 F. V. Dandawate, J. G. Kadolikar, V. D. Kelkar and B. A. Kulkarni, Thermochim. Acta, 241 (1994) 103.
22 S. B. Jagtap, S. G. Joshi, G. M. Litake, V. S. Ghole and B. A. Kulkarni, Metal Based Drugs, 7 (2000) 147.
23 S. B. Jagtap, N. N. Patil, B. P. Kapadnis and B. A. Kulkarni, Metal Based Drugs, 8 (2001) 159.
24 D. D. Perrin, W.L.F. Armarego and D. R. Perrin, 'Purification of Laboratory Chemicals', Pergamon Press, Oxford 1966.
25 L. N. Mulay and I. N. Mulay, Anal. Chem., 44 (1972) 324; B. N. Figgis and J. Lewis in F.A. Cotton (Ed.), Prog. Inorg. Chem., Vol. 6, Interscience, New York 1964 and R. S. Drago, 'Physical Methods in Chemistry', W. B. Saunders Co., Philadelphia 1977 and references therein.
26 B. N. Figgis and J. Lewis in J. Lewis and R. G. Willkinson (Eds), Modern Coordination Chemistry: Principles and Methods, Interscience, New York 1968, p. 403.
27 C. G. Pierpont and R. M. Buchanan, Coord. Chem. Rev., 38 (1981) 45.
28 S. S. Sawhney, R. Jain and J.M.M. Singh, Thermochim. Acta, 132 (1988) 275.
29 S. S. Sawhney and B. M. L. Bhatia, Thermochim. Acta, 43 (1981) 243.
30 W. Berzyska, A. Kula and Z. Rzaezynska, J. Thermal Anal., 47 (1991) 599.
31 R. S. Bottei and C. P. McEchern, J. Inorg. Nucl. Chem., 32 (1970) 2653.
32 V. D. Kelkar, H. R. Gholap, R. R. Gokhale and M. B. Kulkarni, Ind. J. Chem., 37A (1998) 915.
33 A. W. Coats and J. P. Redfern, Nature, 201 (1964) 68.
34 D. A. Anderson and E. S. Freeman, J. Appl. Polym. Sci., 1 (1959) 192.
35 J. H. Van Vleck and N. Frank, Phys. Rev., 34 (1929) 1494, 1625.
36 T. Moeller and E.P. Horowitz, J. Inorg. Nucl. Chem., 12 (1960) 49.
37 D. E. Henrie, Coord. Chem. Rev., 18 (1976) 119.
38 S. P. Sinha, Spectrochim. Acta, 22 (1966) 57.
39 T. R. Rao, I. A. Khan and R. C. Agrawal, J. Ind. Chem. Soc., 63 (1986) 380.
40 R. S. Drago, 'Physical Methods for Chemists', Saunders College Publishing 2nd Edn., 1992.
41 A. Chakravorty, Coord. Chem. Rev., 13 (1974) 1.